水平管群を流下する液膜表面波の生成とガス吸収促進の機構解明

Our preliminary experiments showed that such horizontal wavefronts are hardly formed with diminutive defects in uniform distribution at small *Re*. These observations show that the superior uniform distribution was achieved with the new distributor employed.

3.2. Wave-augmented mass transfer and transition to turbulent flow

The Sherwood number *Sh* of a film about 1 m tall is proportional to *Re* raised to the power of 1.1, 0.5 and 1.25 at the ranges of $Re<40$, $40<Re<400$ and $Re>400$, respectively (Fig. 5-a). The first break of the *Sh–Re* curve at $Re\sim40$ is caused by wavefront distortions associated with the partial wave disintegration into dimples. This observation is in agreement with Park & Nosoko's finding [16] that at $Re>40$, humps increase the wavefront distortion to break the wavefronts into several horseshoe shapes associated with marked deceleration of the mass transfer enhancement. The transition to turbulent flow causes the second break at $Re\sim400$, and this critical value was also determined by Brauer [11] and Feind [23] from measurements of the film thickness and the wall shear stress, respectively.

Bakopoulos' correlations [3] are in excellent agreement with the present measurements for the tall film with natural and forced waves at Re=70–300. At $30<Re<70$, however, the present data are larger than his correlations. The present results suggest that for uniformly distributed films of about 1 m height or taller at $Re<70$, Bakopoulos' correlations may have to be revised to,

an extension of Bakopoulos' second correlation, $Sh=8.0\times10^{-2}Re^{0.5}Sc^{0.5}$ from $Re>70$ to $Re>40$,

and

a new correlation, $Sh=8.8\times10^{-3}Re^{1.1}Sc^{0.5}$ at $20<Re<40$.

The revised correlations pass through or near the upper boundary of Kamei & Oishi's [5] and Hikita et al.'s [4] measurements which supplied the main body of the data for Bakopoulos' first and second correlations, while his existing correlations pass through or near the lower boundary (refer to Fig. 1 in [3]). Kamei & Oishi [5] and Hikita et al. [4] formed films through *overflowing*, and Bakopoulos cited the serious difficulties in obtaining uniform distribution by overflowing especially at low flow rates. Bakopoulos' measurements of the mass transfer in a film discharged from an undulated annular distributor fall on or near the revised correlations and are larger than those in film discharged from a ring slot (refer to Fig. 6 in [3]).

The measurements of *Sh* are larger by approximately 17% for forced waves on the short film of 0.37 m height than the 0.95 m tall film at both ranges of $Re<40$ and $40<Re<300$, though both short and tall films have the same slopes of *Sh* at the both ranges. This may be attributed to the growth of the concentration boundary layer in the films. Miyara's [32] and Nagasaki et al.'s [33] numerical simulations of wavy film flow and diffusion into the film showed that humps have gentle flow circulations in the near-peak regions of the humps, and the flow is rather *smooth laminar* (or not wavy) near the wall under the humps and in the substrate between humps. The

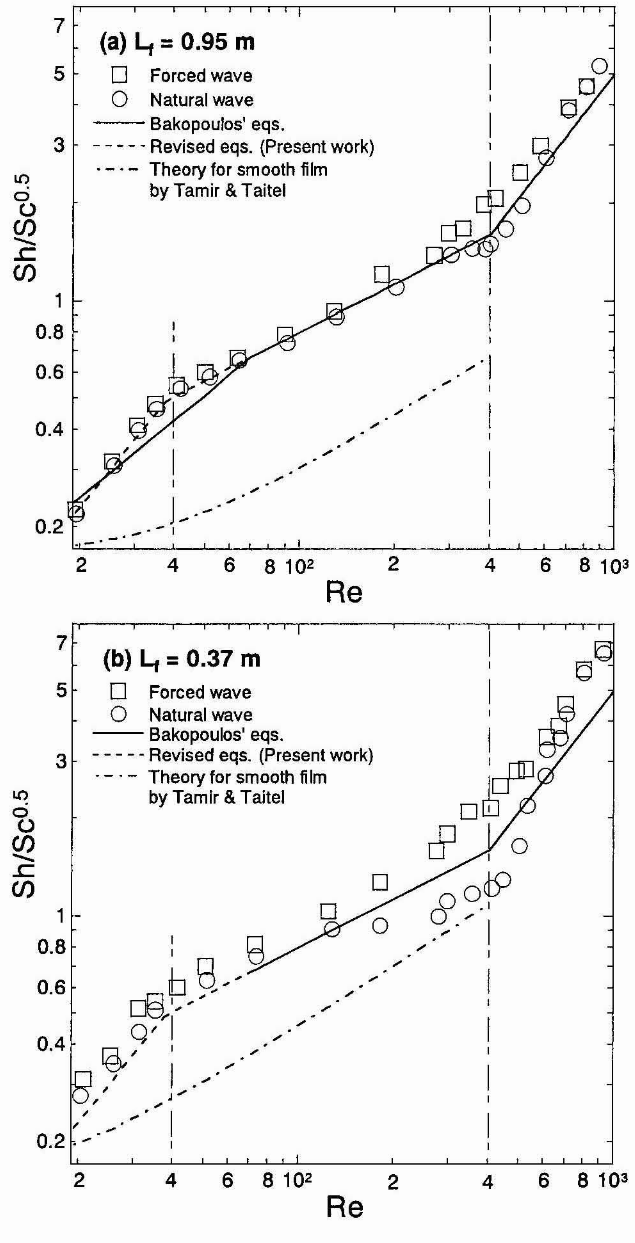

Fig. 5 Variation of *Sh* with *Re* for (a) 0.95 m and (b) 0.37 m tall films. Solutions by Tamir & Taitel [34] to the equation of diffusion in smooth film are presented for comparison, and Bakopoulos' correlations are revised to fit the plots for uniformly distributed film at 20<*Re*<40 and 40<*Re*<70.

hump-induced convections seem to cause partial renewals of the concentration boundary layer at and near the film surface [30], but the layer continuously grow in the near-wall region under humps and between humps, and therefore *Sh* decreases with increasing length of the developing boundary layer, i.e. the film height. The solutions to the diffusion equation in Nusselt film by Tamir & Taitel [34] are much smaller than the measurements of *Sh* for the wavy films at any *Re*, and the solution for the short film is larger than that for the tall film. The wave-induced convections dominate the interfacial mass transfer between the surface and the bulk [30] and the effect of the continuously developing boundary layer is limited to the near wall region, and therefore the measurements of *Sh* are larger for the short film than the tall film only by 17% in spite of the much larger differences in the *Sh* solution between the short and tall flat films.

The present measurements in *Sh* may have a fairly large error at the turbulent-flow range of *Re* though the error is small at the laminar-flow range. The number of bubbles entrained into the water pool greatly increases at the turbulent-flow range, and the bubble separator employed could not remove the bubbles completely. The gas absorption from the bubbles may increase the measurements of C_{out} and *Sh*, and cause deviations of the measurements from the Bakopoulos correlations at the turbulent-flow range (see Fig. 5). The excess absorption from the bubbles has a larger ratio to the absorption through the film surface for a shorter film causing a larger deviation. The deviation is approximately +18% and +34% for forced waves on 0.95 m and 0.37 m tall films having negligible smooth entry passes, respectively, and the same amounts of deviation are observed for the natural waves at $Re>700$ where the smooth entry pass disappears. The slope of *Sh–Re* curve is approximately 1.25 for forced waves on both 0.95 m and 0.37 m tall films at $Re>400$, and the slope itself is in good agreement with that of Bakopoulos' correlation. These observations may agree with Bakopoulos' measurements of *Sh* for 0.45 m and 0.95 m tall films covered with natural waves. The 0.45 m and 0.95 m tall films showed large deviations from his correlation for the turbulent-flow range, and the deviations are much larger than the present ones. The bubble separator installed in our apparatus seemed to reduce the deviation significantly.

In a similar manner to the abrupt increases of the heat and mass transfer observed in wall boundary shear layers, both the 0.37 m and 0.95 m long films covered with natural waves show sharp rises in *Sh* at the transition range of $400<Re<700$ (Fig. 5). Associated with the smooth entry pass shortening rapidly the slope of *Sh* for natural waves is much larger at $400<Re<700$ than the 1.25 slope of Bakopoulos equation. The *Sh* for natural waves catches up with the values for forced waves and then increases with the 1.25 slope at Re~700 or larger. This is more evident for the short film as shown in Fig. 5-b. These sharp rises in *Sh* suggest that in the films with deceleration inlet flow, the laminar developing entry region is not longer than 0.37 m long tube at Re~400, and it rapidly retracts upstream with increasing *Re* at the transition range of $400<Re<700$ in a similar manner to the smooth entry pass (Fig. 4). The developing entry region should be longer than the smooth entry pass since the waves with large surface-height fluctuations that trigger localized turbulences [21], develop downstream of the appearance of dimples. The transition starts at about 400 even in the 0.37 m film with decelerating inlet flow, which is much shorter than the 0.9–1.3 m long laminar developing entry region observed at $370<Re<750$ by Takahama & Kato [13]. Furthermore, the smooth entry pass rapidly shortens on the present films of the decelerating inlet flow with increasing *Re* at $400<Re<700$ (Fig. 4) while its length further stretch out and then levels out on films with the accelerating inlet flow (see Fig. 4 for Tailby & Portalski's [8] curve). These suggest that the decelerating inlet flow triggers the transition to turbulent flow at a further upstream location and makes the *Re* transition range narrower than the accelerating inlet flow.

The inlet forcings might account for a contraction in the transition range of *Re* to a nearly single, sharply defined critical value, and reduce the critical *Re* for the onset of turbulent flow from 400 to about 300. The measurements of *Sh* start to increase rapidly with a slope of 1.25 at $Re\sim300$ for forced waves on both the tall and short films, shifting the second break from $Re=400$ to 300 (Fig. 5). These support the *localized-turbulent flow* in film flow; the inlet forcings trigger the tall humps with long separations to develop shortly downstream of the inlet, and such tall humps may induce localized turbulences under the humps. A shift of the critical *Re* was also observed by Brauer [11]. He showed that a 0.3 mm diameter wire on the tube wall triggers the turbulent flow downstream in a film at $Re=340$ or larger; otherwise the critical *Re* is 400.

The ratio in k_L between a wave-covered film and an entirely flat film may directly show the waves' mass transfer enhancement (Fig. 6). The solutions [34] of k_L to the diffusion equation for Nusselt film has been assumed to be the k_L for the flat film. For films covered entirely with forced waves, the ratio of k_L sharply increases with *Re* at $Re<40$ and then the slope of the ratio curve rapidly decreases beyond $Re\sim40$. The k_L ratio has a local maximum at $Re\sim50$ and then gradually decreases to a local minimum at $Re\sim300$, and then rapidly increases at the turbulent-flow range. The ratio is larger for the taller film, and the local maximum is approximately 2.7 and 2.2 for the tall and short films, respectively. The ratio is smaller for the natural waves than for the forced waves because of the smooth entry pass and the laminar developing entry region preceding the downstream region covered with natural waves, and the difference in the k_L ratio between the forced and natural waves is larger for the short film since the entry pass and the laminar region have larger fractions of their lengths to the film height on the short film. The ratio for the natural waves has the local minimum at $Re\sim400$, and then sharply rises to catch up that for forced waves at $Re\sim700$ or larger.

The deviation in *Sh* of natural waves from forced waves at the laminar-flow range (Fig. 5) is attributed largely to the smooth entry pass. The Sherwood number Sh_{nt} for natural waves with respect to Sh_{fc} for forced waves increases with the length (L_f–L_{sm}) of the wavy region downstream of the wave inception (Fig. 7), though the length scatters widely. The linear correlation fitting the plots is extrapolated to fall within the range of the solutions for the flat film Sh_N plotted at

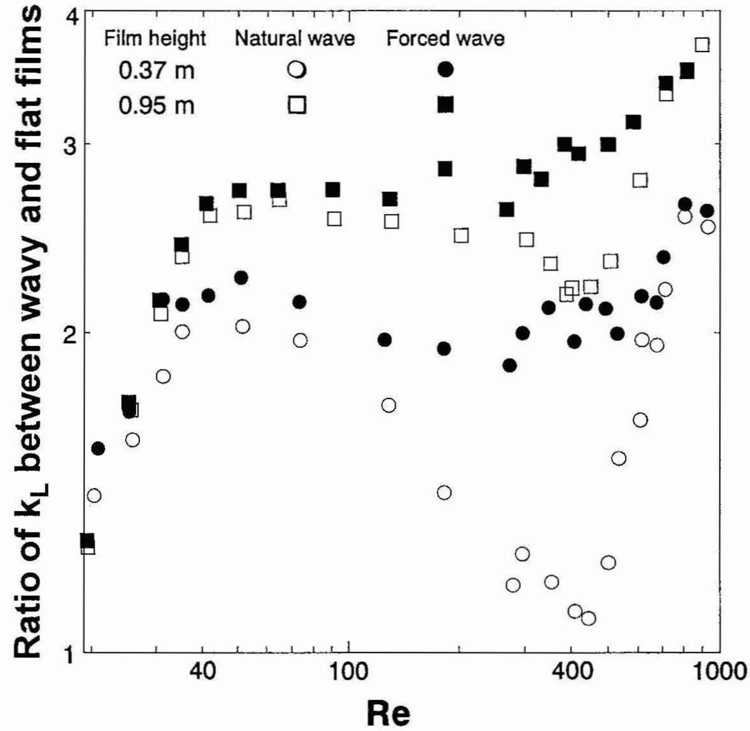

Fig. 6 Variation of mass transfer enhancement with *Re* for 0.95 m and 0.37 m tall films covered with natural waves or forced waves. Ratios of k_L are presented between solutions [34] for flat film and measurements for wavy films.

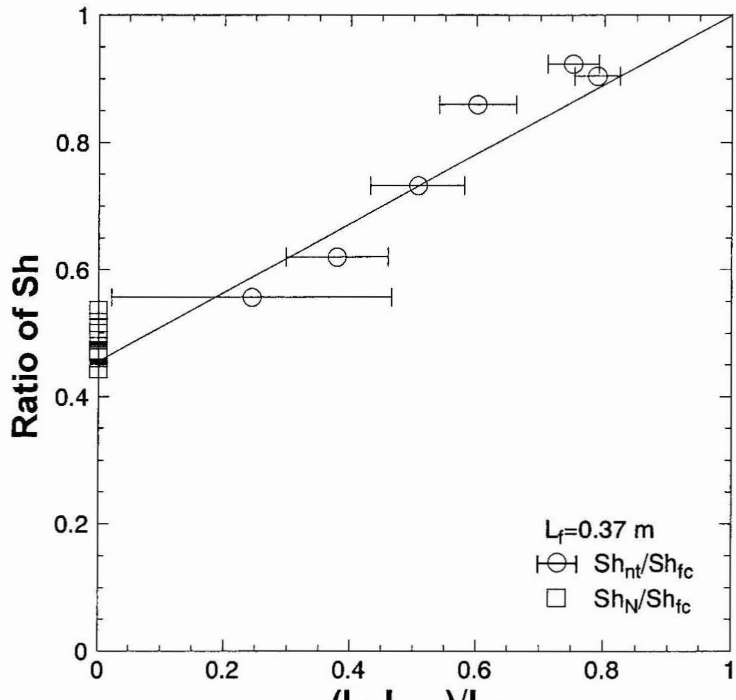

Fig. 7 Length ($L_f - L_{sm}$) of wavy region on film and variation of the ratio, Sh_{nt}/Sh_{fc}, between natural waves and forced waves for 0.37 m tall film at $40<Re<400$. The horizontal bars through plots represent the scattering in the length L_{sm} of the smooth entry pass (see Fig. 4), the fitting line is made by the method of least squares, and the ratio, Sh_N/Sh_{fc}, between solutions for smooth film and measurements for forced waves are plotted at vanishing ($L_f - L_{sm}$).

vanishing length (L_f–L_{sm}). At low *Re* of 40 around, the (L_f–L_{sm})/L_f is nearly unity and the plots of *Sh* ratio are slightly larger than the linear correlation. At high *Re* close to 400, the (L_f–L_{sm}) is close to zero and the plots of *Sh* ratio are smaller than the correlation. These suggest that humps with less distorted wavefronts which appear at the low *Re*, enhance the mass transfer by a factor of larger number than humps with greatly distorted wavefronts accompanying dimples which appear at the high *Re*.

The 9.6 mm diameter of the present small tube may not have noticeable effect on the mass transfer. At the laminar flow range of *Re*, the present measurements are in good agreement with Bakopoulos [3] correlation (Fig. 5), and Bakopoulos constructed the correlations at laminar and turbulent flow ranges mainly from the data of Kamei & Oishi [5] for 47.6 mm inner diameter tube, Hikita et al. [4] for 27 mm inner diameter and Lamourelle & Shandall [6] for 16 mm outer diameter, respectively. Though our data have a 17% deviation from Bakopoulos correlation at the turbulent-flow range (Fig. 5-a), such deviation should be attributed to the excess absorption from bubbles pulled into the water as described above, but not to the small diameter.

3.3. Effects of forcing frequency and tube inclination

The inlet forcings make the smooth entry pass to vanish and increase the mass transfer greatly in short films. For both 0.37 m and 0.69 m tall films the amount of increase in the mass transfer changes with the frequency of the inlet forcings within small margins (Fig. 8). Yoshimura et al. [30] showed that humps triggered by the inlet forcings hold their wavefronts roughly horizontal at *Re*<55 on a 0.24 m tall film and the mass transfer enhancement by such two-dimensional humps changes with the forcing frequency within 15%. The forced waves were observed to critically increase the wavefront distortion at further downstream distances beyond x=0.24 m at larger *Re* (see Fig. 2-b and refer to [16]). The present results suggest that the frequency of such humps with distorted wavefronts changes the mass transfer enhancement within small margins.

A tube inclination from the vertical makes the hump wavefronts slant as they travel downstream (Fig. 3-b). The partial disintegrations into dimples are fixed to the upper ends of the slanting wavefronts where the resulting dimples are released upstream, and dark strips representing hump wavefronts are observed more evidently. The wavefronts slant less rapidly at the turbulent-flow range of *Re* than the laminar-flow range (Fig. 3-b). The *Sh* decreases with the tube inclination, and the decrease in *Sh* is more serious in the laminar-flow films than the turbulent-flow films, and is also true for taller films (Fig. 9). For a 0.68 m tall film, a 0.5^{o} inclination causes decreases in *Sh* by 10–20% and by 4% in the laminar and turbulent flows, respectively.

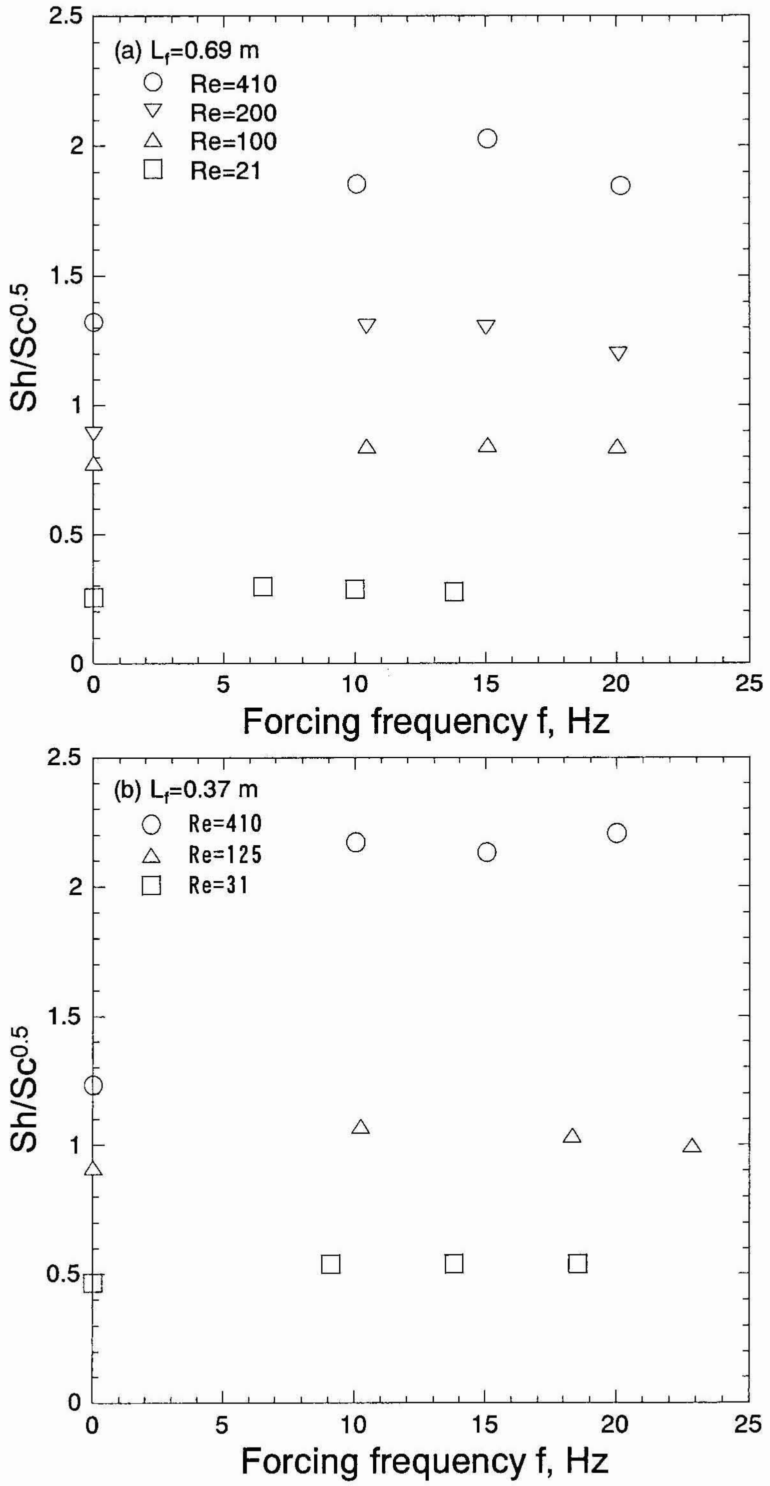

Fig. 8 *Sh* variations with forcing frequency *f* for (a) 0.69 m and (b) 0.37 m tall films.

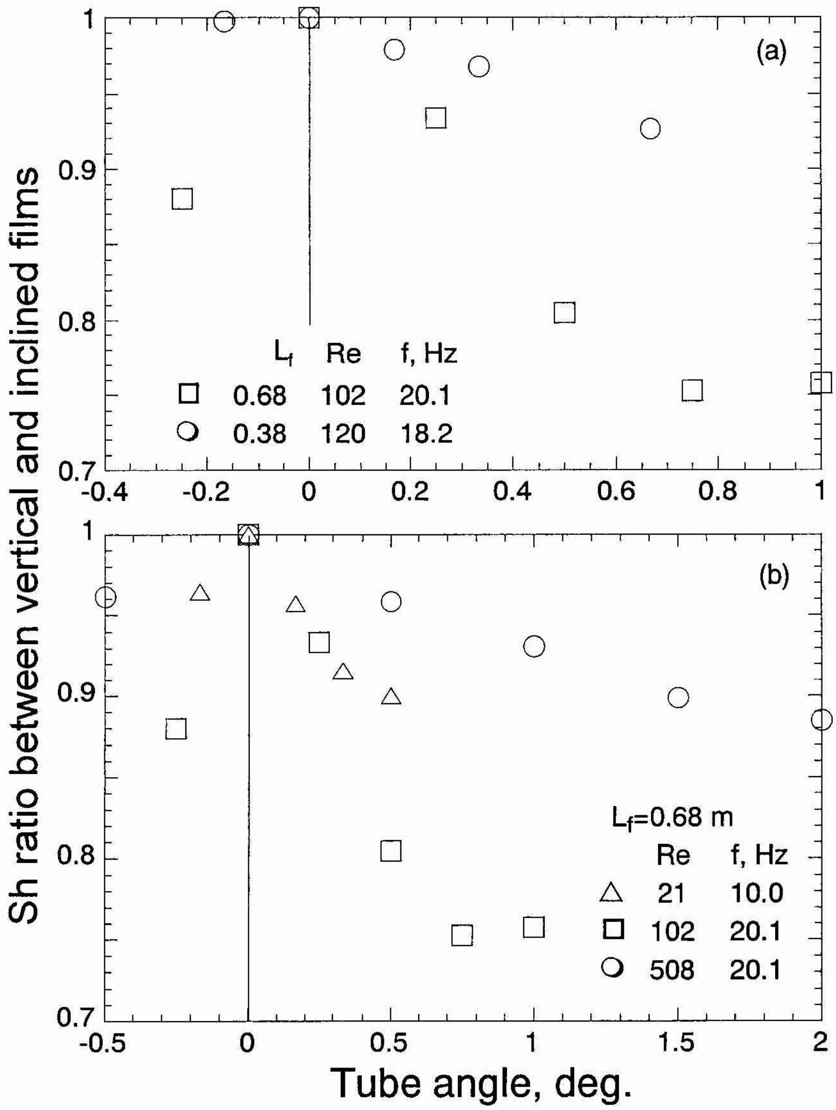

Fig. 9 Mass transfer reductions caused by tube inclination θ from the vertical: comparisons are presented (a) between 0.38 m and 0.68 m tall films, and (b) between films of laminar and turbulent flow.

4. Summary and discussion

In the film flow, the structure of turbulent flow and the transition from *wavy-laminar* to *turbulent* flow have not been fully understood. *Localized-turbulent flow* has been assumed by several researchers after Jackson [35]; turbulences are localized under large waves traveling on a thin substrate in which the flow is laminar otherwise. Recently Karimi & Kawaji [21,22] detected such localized turbulence under large waves at far downstream distances from the film inlet by rapid diffusion of laser-induced photochromic dye tracers. By the breaks appearing in curves of the mean film thickness vs. *Re*, Takahama & Kato [13] determined the laminar developing entry region whose length decreases with increasing *Re* at the transition range. On the other hand, from measurements of the mass transfer, single critical Reynolds numbers have been determined by breaks in curves of the mean mass transfer coefficient k_L or *Sh* vs. *Re*, instead of *Re ranges* [3,5,7]. To our knowledge, the transition *range* of *Re* or the laminar developing entry region was first evidently captured on measurements of the mass transfer in the present work. Though the measurement error in *Sh* is fairly large at the transition and turbulent-flow ranges, the comparisons of the *Sh*–*Re* curve between natural waves and forced waves and between the tall and short films evidently showed the sharp rises in *Sh* at the transition range of *Re*, suggesting that the laminar developing entry region rapidly shortens at the transition range. Comparison of the present results with Takahama & Kato's [13] indicates that the length of the laminar developing region and the transition range of *Re* are sensitive to the inlet flow conditions.

For practical applications of the interfacial mass transfer processes, low flow rates of $40<Re<100$ are recommended in falling water films, at which the maximum mass transfer enhancement or near-maximum enhancement is available with low pumping power (Fig. 6), though Roberts & Chang [2] recommended the flow rates of $Re\sim40$ based on their theoretical model analysis. To achieve uniform distribution at such low flow rates, the authors recommend the use of the feeding device employed in this work or one similar to it, i.e. 'undulated annular distributor' used by Brauer [19] and Bakopoulos [3]. Tubes should be aligned to be strictly vertical; otherwise for 0.7 m or taller films, a 0.2° inclination may cause 5% or larger reductions in mass transfer coefficient (Fig. 9). The inlet forcings are most effective when these are applied to short films at $150<Re<600$ where the smooth entry pass and the laminar developing entry region have large fractions of their lengths to the film height. The forcings drastically shorten the smooth entry pass and the laminar developing region to enhance the mass transfer, though the enhancement changes with the frequency of the forcings within small margins.

Reference

[1] S.V. Alekseenko, V.E. Nakoryakov, B.G. Pokusaev, Wave flow of liquid films, Begell House Inc., New York, 1994.

[2] R.M. Roberts, H.-C. Chang, Wave enhanced interfacial transfer, Chem. Eng. Sci. 55 (2000) 1127-1141.
[3] A. Bakopoulos, Liquid-side controlled mass transfer in wetted-wall tubes, Ger. Chem. Engng, 3 (1980) 241-252.
[4] H. Hikita, K. Nakanishi, T. Kataoka, Chemical Engineering (Japan) 23 (1959) 459-466.
[5] S. Kamei, J. Oishi, Mass and Heat Transfer in a falling liquid film of wetted wall tower, Memoirs of the Faculty of Eng., Kyoto Univ. 17 (4) (1955) 277-284.
[6] A.P. Lamourelle, O.C. Sandall, Gas absorption into a turbulent liquid, Chem. Eng. Sci. 27 (1972) 1035-1043.
[7] R.E. Emmert, R.L. Pigford, A study of gas absorption in falling liquid films, Chem. Eng. Progress 50 (1954) 87-93.
[8] S.R. Tailby, S. Portalski, Wave inception on a liquid film flowing down a hydrodynamically smooth plate, Chem. Eng. Sci. 17 (1962) 283-290.
[9] G.D. Fulford, The flow of liquids in thin films, in Advances in Chemical Eng. 5 (Academic Press, New York, 1964) 151-236.
[10] S. Portalski, A.J. Clegg, An experimental study of wave inception on falling liquid films, Chem. Eng. Sci. 27 (1972) 1257-1265.
[11] H. Brauer, Stromung and Warmeubergang bei Rieselfilmen, VDI (Ver. Deut. Ingr.) - Forschungshelt, **457** (1956).
[12] D.R. Webb, G.F. Hewitt, Downwards co-current annular flow, Int. J. Multiphase Flow 2 (1975) 35-49.
[13] H. Takahama, S. Kato, Longitudinal flow characteristics of vertically falling liquid films without concurrent gas flow, Int. J. Multiphase Flow 6 (1980) 203-215.
[14] R.P. Salazar, E. Marschall, Time-average local thickness measurement in falling liquid film flow, Int. J. Multiphase Flow 4 (1978) 405-412.
[15] T.D. Karapantsios, A.J. Karabelas, Longitudinal characteristics of wavy falling films, Int. J. Multiphase Flow 21 (1) (1995) 119-127.
[16] C.D. Park, T. Nosoko, Three-dimensional wave dynamics on a falling film and associated mass transfer, AIChE J. 49 (2003) No. 11 (*in Press*).
[17] K.J. Chu, A.E. Dukler, Statistical characteristics of thin, wavy films, Part III. Structure of the large waves and their resistance to gas flow, AIChE J. 21 (1975) 583-593.
[18] H.-C. Chang, E.A. Demekhin, E. Kalaidin, Simulation of noise-driven wave dynamics on a falling film, AIChE J. 42 (1996) 1553-1568.
[19] H.-C. Chang, E.A. Demekhin, E. Kalaidin, Y. Ye, Coarsening dynamics of falling-film solitary waves, Physical Review E 54 (1996) 1467-1477.
[20] H.-C. Chang, E.A. Demekhin, S.S. Saprikin, Noise-driven wave transitions on a vertically falling film, J. Fluid Mech. 462 (2002) 255-283.
[21] G. Karimi, M. Kawaji, An experimental study of freely falling films in a vertical tube, Chem. Eng. Sci. 53 (1998) 3501-3512.
[22] G. Karimi, M. Kawaji, Flow characteristics and circulatory motion in wavy falling films with and without counter-current gas flow, Int. J. Multiphase Flow 25 (1999) 1305-1319.
[23] K. Feind, Strömungsuntersuchungen bei Gegenstrom von Rieselfilmen und gas in lotrechten Rohren, VDI-Forschungsheft. 481 (1960).
[24] W. Wilke, Wärmeübergang an Rieselfilme, VDI (Ver. Deut. Ingr.)-Forschungshelt, 490 (1962).
[25] H. Brauer, H. Thiele, Chem. –Anlagent Verfahren (1975) Nr.4, 28-30 (reported in ref. [3]).
[26] W. Malewski, Chem. –Ing. –Tech. 40 (1968) 201-206 (reported in ref. [3]).
[27] F.W. Pierson, S. Whitaker, Some theoretical and experimental observations of the wave structure of falling liquid films, Ind. Eng. Chem., Fundam. 16 (4) (1977) 401-408.
[28] G.A. Truesdale, A.L. Downing, G.F. Lowdan, The solubility of oxygen in pure water and sea-water, J. Appl. Chem. 5 (1955) 53-62.
[29] T. Nosoko, P.N. Yoshimura, T. Nagata, K. Oyakawa, Characteristics of two-dimensional waves on a falling liquid films, Chem. Eng. Sci. 51 (1996) 725-732.
[30] P.N. Yoshimura, T. Nosoko, T. Nagata, Enhancement of mass transfer into a falling laminar liquid film by two-dimensional surface waves (Some experimental observations and modeling), Chem. Eng.

Sci. 51 (1996) 1231-1240.
[31] F.P. Stainthorp, J.M. Allen, The development of ripples on the surface of a liquid film flowing inside a vertical tube, Trans. Instn Chem. Engrs. 43 (1965) T85-T91.
[32] A. Miyara, Numerical simulation of wavy liquid film flowing down on a vertical wall and an inclined wall, Int. J. Thermal Sciences 39 (2000) 1015-1027.
[33] T. Nagasaki, H. Akiyama, H. Nakagawa, Numerical analysis of flow and mass transfer in a falling liquid film with interfacial waves, Thermal Sci. & Eng. 10 (2002) 17-23.
[34] A. Tamir, Y. Taitel, Diffusion to flow down an incline with surface resistance, Chem. Eng. Sci. 26 (1971) 799-808.
[35] L.J. Jackson, Liquid films in viscous flow, AIChE J. 1 (1955) 231-240.